

Configuration of the ASTRI telescopes in *sim_telarray* for the simulation of the CTA pre-production phase (Prod3).

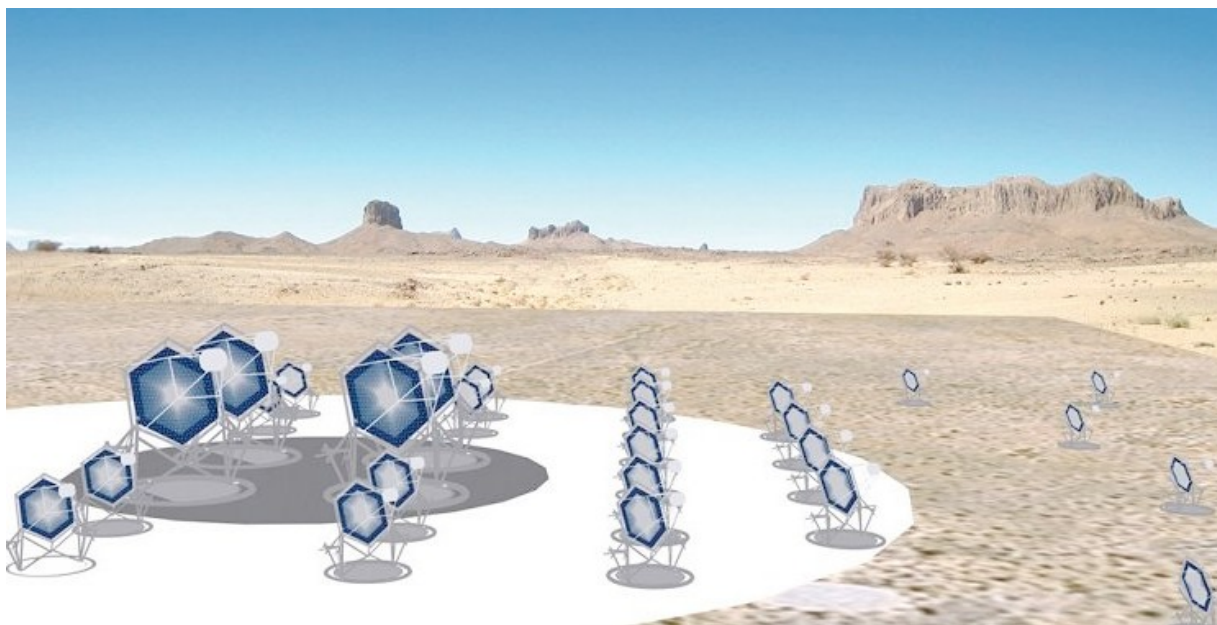
F. Di Pierro¹, C. Bigongiari¹, G. Bonanno², G. Bonnoli³, R. Canestrari³, O. Catalano⁴, G. Cusumano⁴, D. Impiombato⁴, V. La Parola⁴, G. Pareschi³, G. Romeo², A. Stamerra¹, P. Vallania¹.

¹ INAF, Osservatorio Astrofisico di Torino

² INAF, Osservatorio Astronomico di Catania

³ INAF, Osservatorio Astrofisico di Brera

⁴ INAF, IASF Palermo



Prepared by: Name: Federico Di Pierro Signature: _____ Date: _____

Reviewed by: Name: _____ Signature: _____ Date: _____

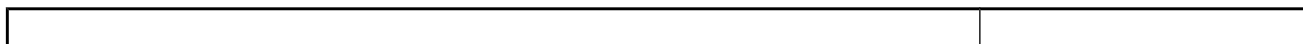
Approved by: Name: _____ Signature: _____ Date: _____

--	--



TABLE OF CONTENTS

DISTRUBUTION LIST.....	3
LIST OF ACRONYMS.....	3
INTRODUCTION.....	4
SIMULATION OF THE OPTICS.....	5
SIMULATION OF THE CAMERAAND THE ELECTRONICS.....	10
CONCLUSIONS.....	14
REFERENCES.....	15





DISTRUBUTION LIST

ASTRI distribution list

astri@brera.inaf.it

LIST OF ACRONYMS

Prod3 = third CTA MC WP large scale production

CTA = Cherenkov Telescope Array

M1 = Mirror 1, ASTRI primary mirror

SiPM = Silicon Photomultiplier

PDE = Photo Detection Efficiency

NSB = Night Sky Background

SST = Small Size Telescope

--	--



INTRODUCTION

In this document we list the configuration parameters and describe the implementation of the ASTRI telescopes in the *sim_telarray* simulation software [1-3] for the CTA third MC production (Prod3). The main aim of Prod3 is the optimization of the CTA layout and we want to implement our best knowledge of the telescopes as they will be in the pre-production phase.

SIMULATION OF THE OPTICS

We implemented the ASTRI Optical Design accordingly to [4]. The primary mirror is segmented in 18 hexagonal tiles, the secondary mirror is monolithic and the shadowing due to the M2 supporting structure, the optical baffle, the camera body are directly simulated. To reduce the simulation time the 12 tubes constituting the mast are considered as an average, incidence angle dependent, telescope transmission parameter. The reflectivity of both mirrors are included separately and the effects of the protective PMMA window are also considered.

Graph

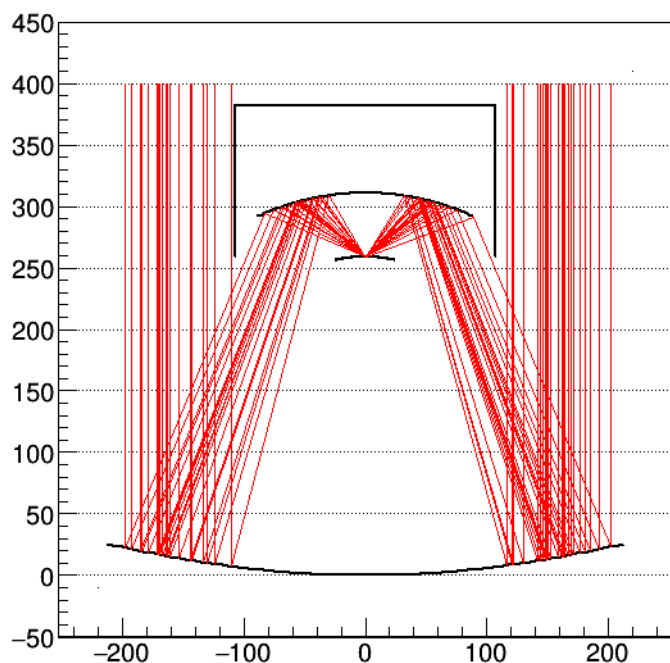


Fig. 1 ASTRI general optical layout.

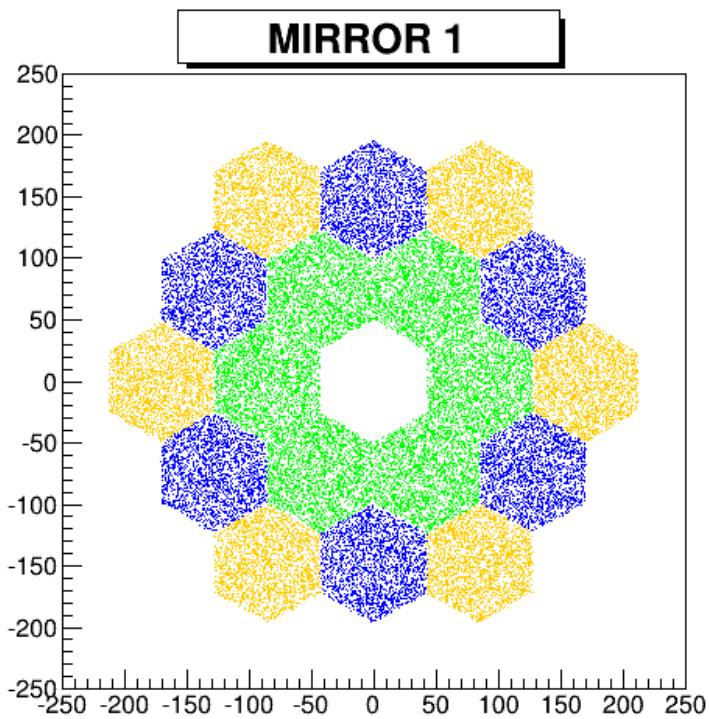


Fig.2 The 18 mirror tiles of the primary mirror.

Graph

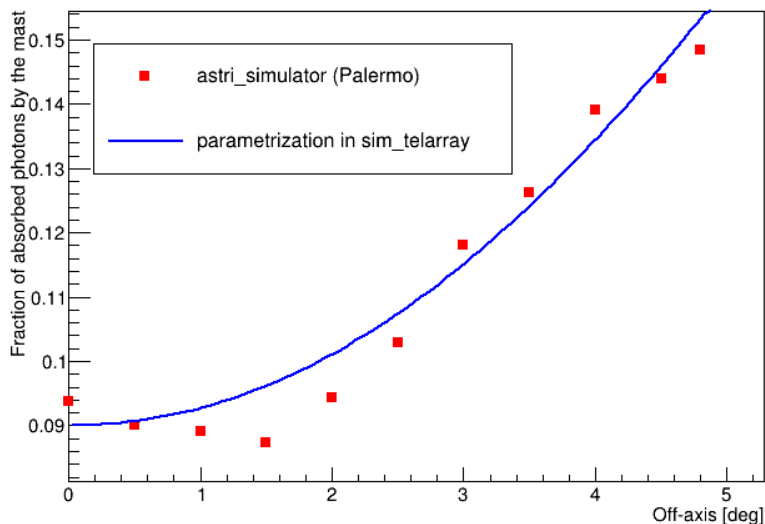


Fig. 3 Fraction of photons absorbed by the mast (12 tubes) as a function of off-axis angle. In sim_telarray: "telescope_transmission".

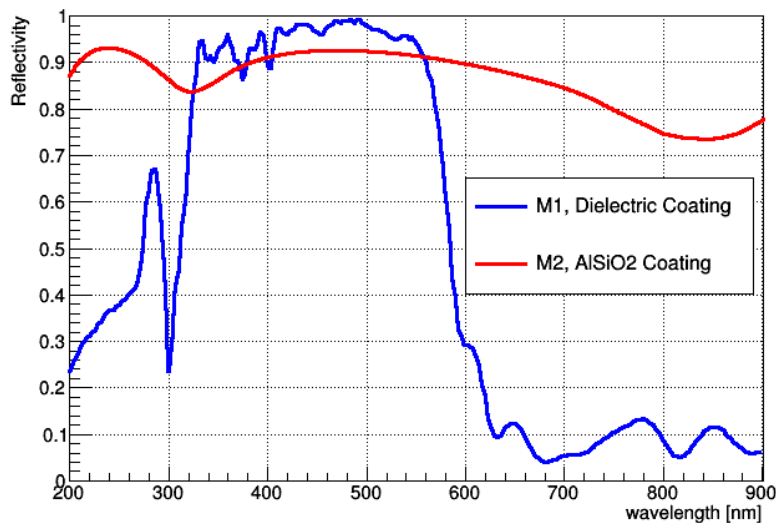


Fig.4 Primary and secondary mirror reflectivities.

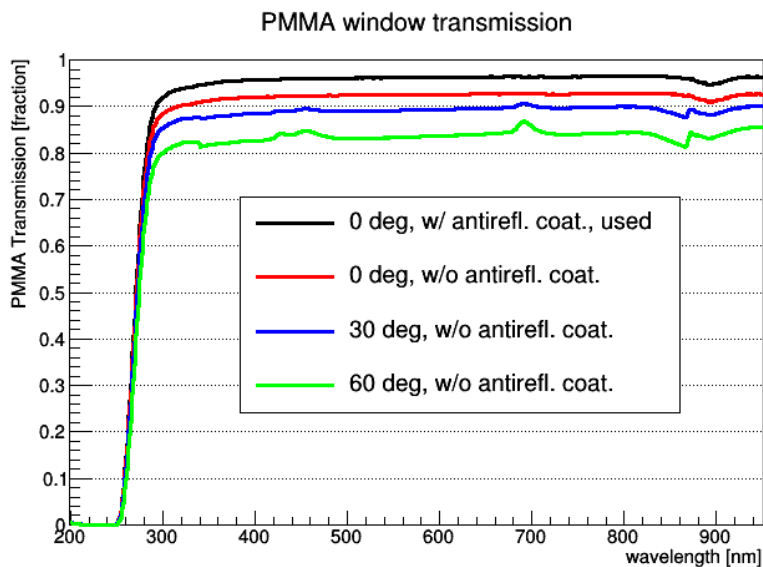
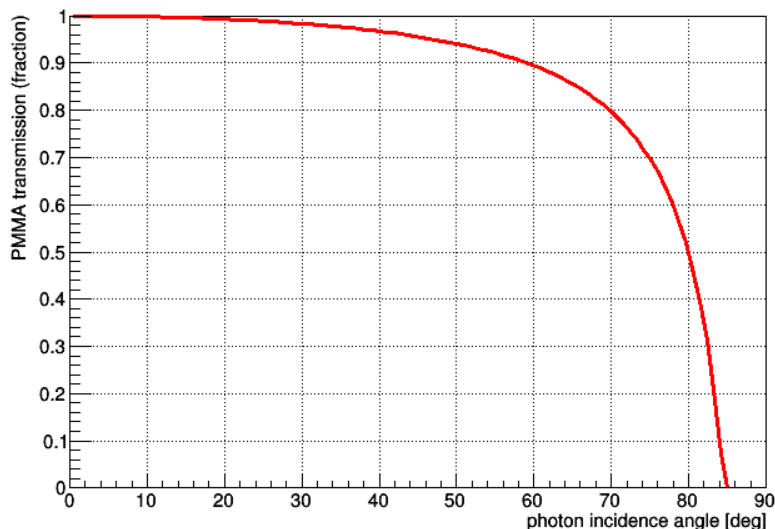


Fig. 5 Measured transmittivity of the PMMA camera window as a function of the wavelength and for different photon incidence angles. The black one includes also the effect of the antireflection coating and it is used.



*Fig. 6 Model of relative transmission of the PMMA window as a function of the photon incidence angle. The final PMMA transmission is: $trans(wl,theta) = trans_1(wl) * trans_2(theta)$.*

The configuration card

```
% ----- Optical parameters -----
mirror_class = 2

primary_mirror_parameters =
0.,0.000608051,-7.36248e-10,5.82125e-15,-6.76447e-20,-3.89542e-24,-5.28036e-29,2.99107e-3
4,4.39153e-38,6.17433e-43,-2.73586e-47

primary_ref_radius = 1

secondary_mirror_parameters =
310.84,0.00229358,2.8273e-08,-2.7689e-12,8.80066e-17,3.37315e-21,-1.02973e-25,-6.72882e-
30,-3.06437e-34,3.1718e-38,-3.71217e-43

secondary_ref_radius = 1

focal_surface_parameters = 258.88, -0.00471698, -1.04952e-07, -4.67036e-12, -2.59788e-16,
-1.61847e-20, -1.08033e-24, -7.55454e-29, -5.46285e-33, -4.0516e-37, -3.06502e-41

focal_surface_ref_radius = 1

focal_length = 215.0

primary_diameter = 430.6
```




```
secondary_diameter = 180.0
primary_segmentation = astri_M1_segments.dat
random_focal_length = 0.0
mirror_reflection_random_angle = 0.0 %ideal psf
%mirror_reflection_random_angle = 0.0075 %realistic psf
mirror_align_random_distance = 0.0
mirror_align_random_horizontal = 0.0
mirror_align_random_vertical = 0.0
mirror_offset = 0.0 % 0.: Axes crossing at dish center.
focus_offset = 0.0
```

% Reflectivities

```
mirror_reflectivity = inaf_m1_refl_multilay_meas.dat
mirror_secondary_reflectivity = inaf_m2_refl_alsio2_32deg_sim.dat
```

%shadowing

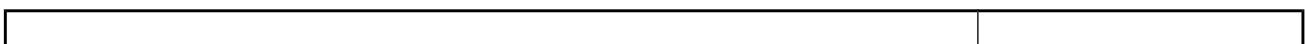
```
camera_body_diameter = 56.0 % cm
camera_depth = 49.0 % cm
secondary_shadow_diameter = 214.0 % [cm] can differ from actual secondary
secondary_shadow_offset = 71.44 % [cm] Actual shadowing from a plate behind secondary
secondary_baffle = 382.28,258.88,107.,0. % z1, z2, R, dR for open cylinder
```

% Telescope transmission angle dependence of function 1:

```
% T(theta) = p0 / (1.+p2*(sin(theta)/p3rad)^p4) with p3rad = p3*pi/180.
telescope_transmission 0.91 1 0.0296 3.037 2.07 %
```

% Accuracy of the tracking and measurement of current direction.

```
telescope_random_angle = 0.
telescope_random_error = 0.
random_viewing_ring = 0.
```



SIMULATION OF THE CAMERA: PHOTSENSORS AND ELECTRONICS

In fig. 7a the 3D geometry of the ASTRI camera is shown and in fig7b its projection on the XY plane (full and zoomed PDM 19, in red PDM 1), with pixels of $6.975 \times 6.975 \text{ mm}^2$.

Graph2D

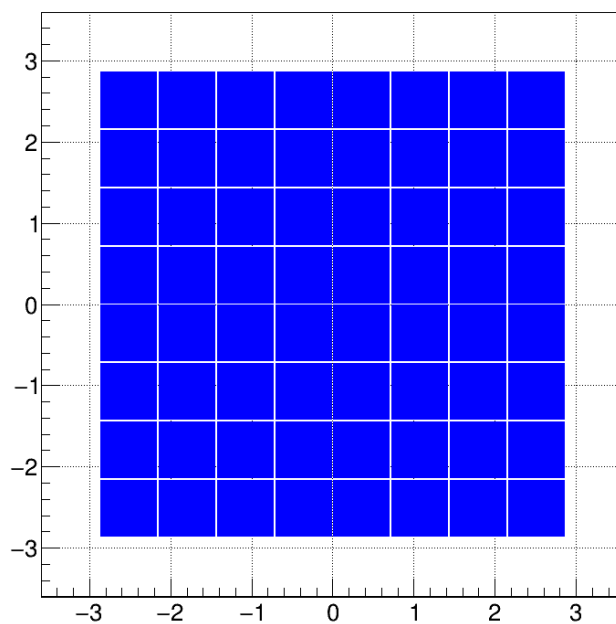
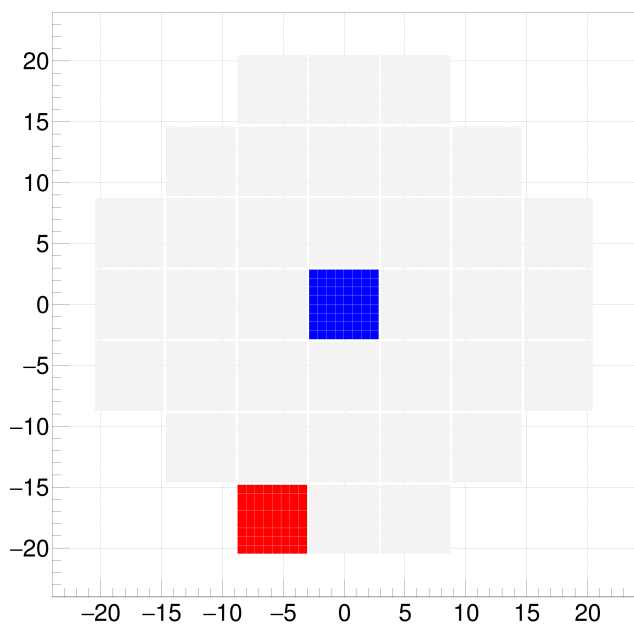
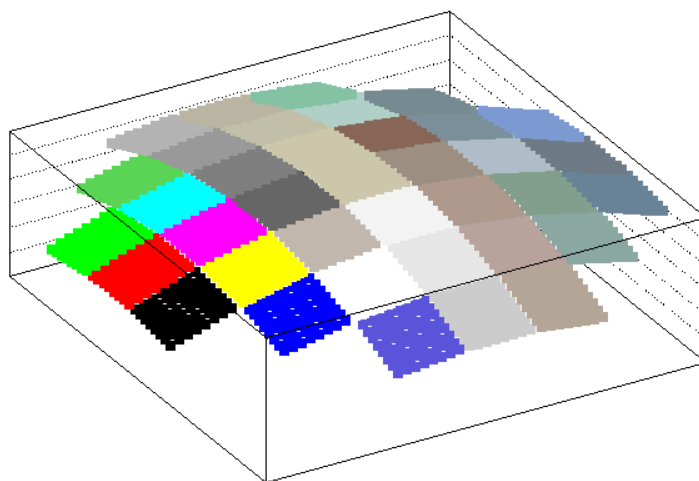
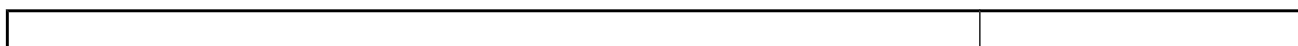


Fig. 7 Geometry of the ASTRI camera. In red PDM 1, in blue PDM 19 (zoomed right panel)



The Photon Detection Efficiency is shown in fig.8a .

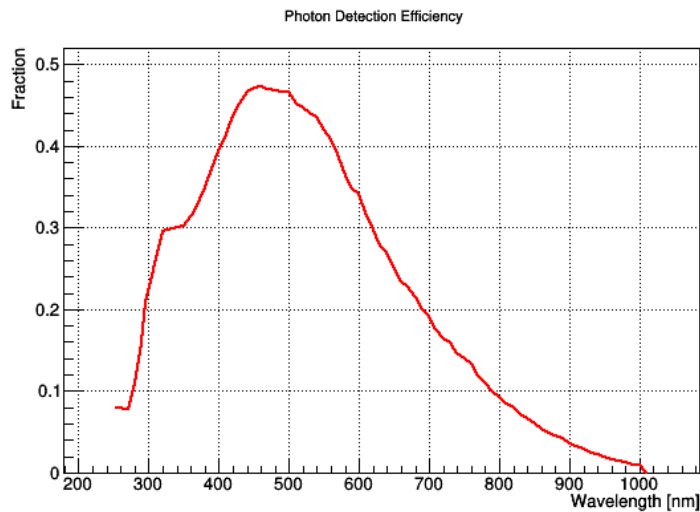


Fig.8a Photon Detection Efficiency (LCT5, 75 μ m, OV = 4V, temperature 15 $^{\circ}$ C).

The SiPM PDE can be considered constant with respect to photon incidence angle, once unfolded from the geometrical effect, as shown in fig. 8b (directly considered in our simulation).

MPPC LCT4 75 μ m Photon flux versus angle of incidence preliminary results

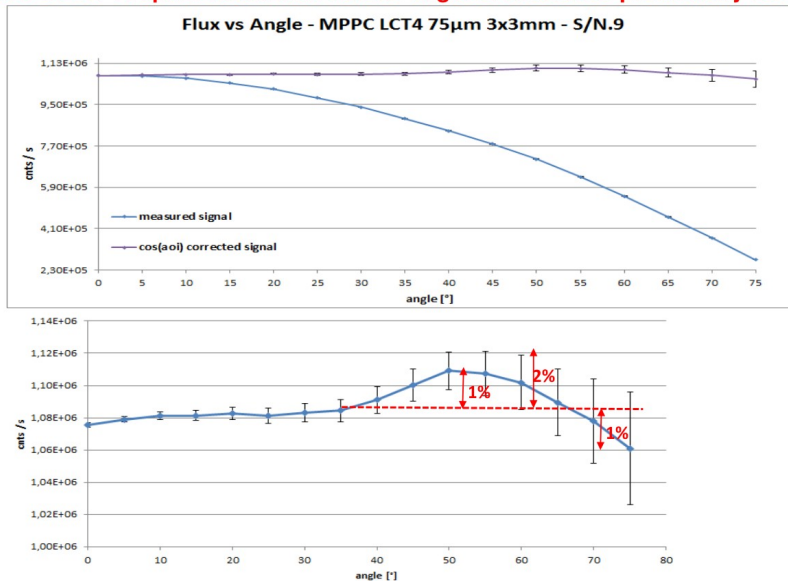


Fig. 8b PDE versus photon incidence angle. (from G. Bonanno, ASTRI GM Bologna 2015)

We extract several information related to the device and the electronics to be simulated, from real calibration events (e.g.: the illumination of the SiPM with a LED, fig. 9). From the shown fit we can extract the values of: baseline, baseline fluctuations, cross-talk, conversion factor between Pe and ADC (gain) and gain fluctuations.

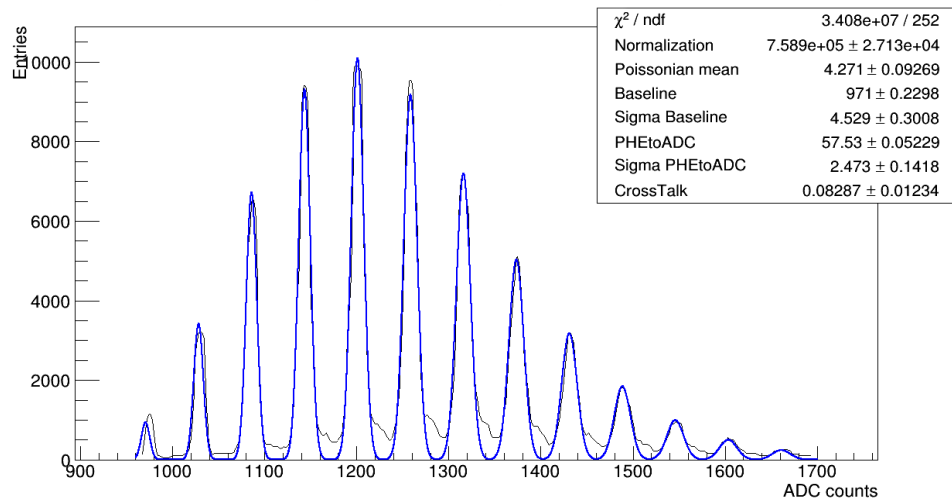


Fig. 9 Calibration events (C1,4) for the new devices and our fitting model (blue curve).

This information is translated into sim_telarray configuration parameters. One of these parameters is the *single photoelectron spectrum*, which includes the gain fluctuations and the cross-talk and it is normalized to mean = 1 and area = 1 (fig.10).

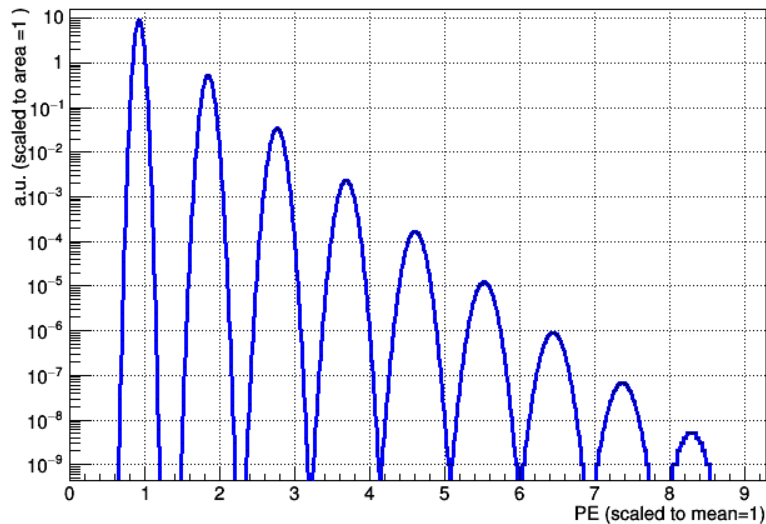


Fig. 10 Single photoelectron spectrum.

Using the obtained set of parameters we reproduce the calibration events (fig.11), simulating the illumination of the camera by a LED.

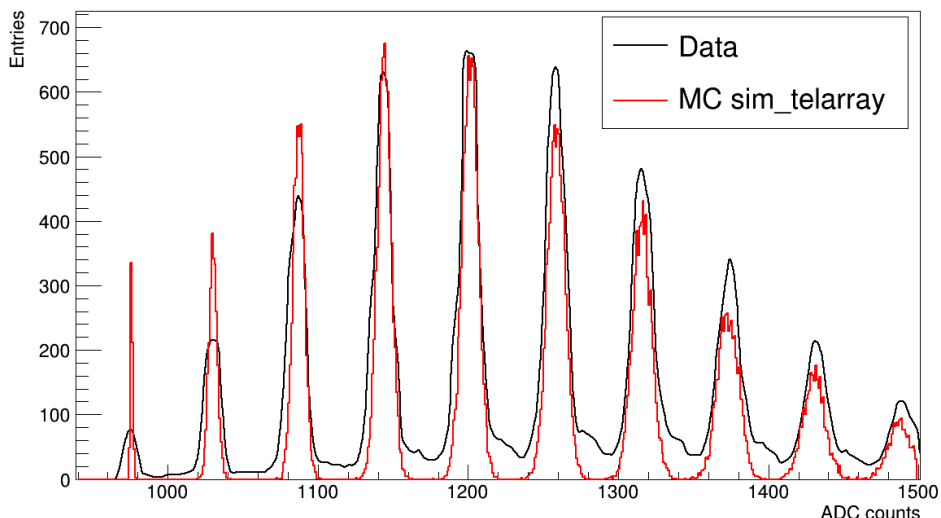


Fig. 11 Calibration events: real and simulated data.

In order to correctly translate the fit parameters to the simulation software input we have to use the information about the SiPM signal integration time, performed by the CITIROC ASIC, which is 37.5 ns (configurable) continuous sliding window. We have tested our simulation of CITIROC and we have found that our results are equivalent to those obtained applying the Laplace transformate to the circuit transfer function.

The readout signal is formed by adding in every time slice the contributions of the signals generated by all photoelectrons (either nsb and cherenkov ones). The used pulse shape relative to 1 pe is shown in fig.12 and its amplitude is fluctuated in order to reproduce measured single photoelectron fluctuations.

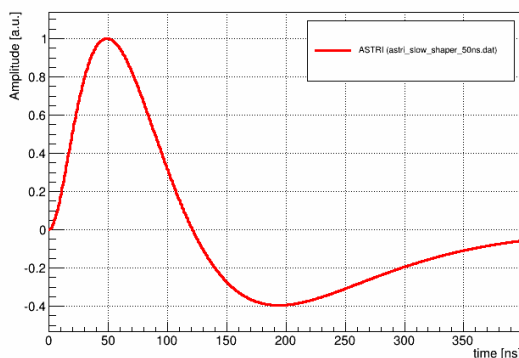


Fig. 12 Readout signal (CITIROC slow shaper, HG)

Finally the simulation code, reproducing the CITIROC readout, provides as output the maximum ADC value of each signal in the simulated time window (240 ns, sampled at 500 MHz), for both HG and LG chains.

The trigger signal is produced similarly, but using a different pulse shape for the single pe (fig.13).

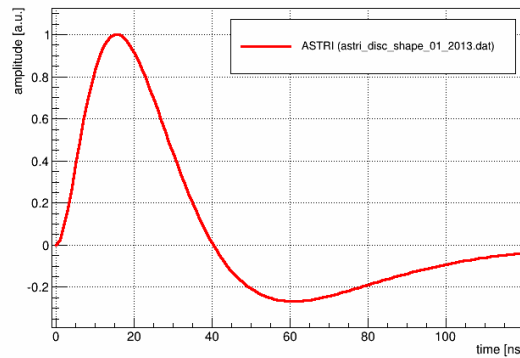


Fig. 13 Discriminator input (EASIROC fast shaper)

The pixel provides a trigger if its *trigger* signal is above a threshold (and with also conditions on time over threshold and signal over threshold). The camera trigger requires 5 adjacent pixels (the triggering combinations are defined in the camera configuration file).

Nightsky background

The value for the NSB pe rate at pixel level must be evaluated considering the nsb spectrum, optics (effective mirror area, reflectivities, protective window), pde, pixel size, as discussed in [5].

With present configuration files the individual pixel pe rate is 44 MHz.



The configuration card

% ----- Camera ASTRI: geom, trig, photosensors -----

pixels_parallel = 0

camera_config_file = camera-astri-smart5-prod3.dat

camera_pixels = 2368 % needs to be specified explicitly

quantum_efficiency= PDE_ASTRI_LCT5_75um_OV_4V_meas.dat % PDE vs lambda

pm_collection_efficiency = 1.

qe_variation = 0.02 % [fraction]

pm_voltage_variation = 0. % [fraction] default 0.03

pm_transit_time = 1. % [ns] default 20.

transit_time_jitter = 0.05 % [ns].

pm_photoelectron_spectrum = SPEspectrum_57.50_2.500_0.080.dat %

nightsky_background = all: *TBD* %GHz pixel, including Dark Counts

% ----- Trigger Signal-----

% simulated time window [ns] = es.: $\text{disc_bins} * \text{fadc_mhz}^{-1} * 1000 = 120 * 500^{-1} * 1000 = 240$ [ns]

% discriminator input:

disc_bins = 120 % Number of time intervals simulated for trigger.

disc_start = 0 % How many intervals the trigger simulation starts before the ADC. default 0

disc_ac_coupled = 1 % default 1

discriminator_pulse_shape = astri_disc_shape_01_2013.dat % ampl. vs time [ns]

discriminator_amplitude = 1.08696 % arb.u.

discriminator_time_over_threshold = 10 % ns, default 1.5

discriminator_var_time_over_threshold = 0.0 % ns, default 0.1

discriminator_sigsum_over_threshold = 0.0 % [mV*ns], default 0.0

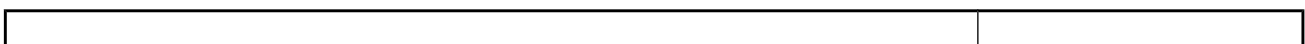
discriminator_var_sigsum_over_threshold = 0.0 % [mV*ns], default 0.0

discriminator_threshold = *TBD* % [same as discriminator_amplitude] $5\text{pe} * 1.08696 = 5.43$

discriminator_var_threshold = 0.0 % channel-to-channel variation

%discriminator output:

discriminator_gate_length = 20.0 % ns, default 2.0





discriminator_var_gate_length = 0.0 % ns, default 0.1
discriminator_output_amplitude = 1.0 % arb. units
discriminator_output_var_percent = 5 % is 10% for HESS
discriminator_rise_time = 0.5 % [ns] is 1ns for HESS
discriminator_fall_time = 0.5 % [ns] is 1ns for HESS

%---- camera trigger:

default_trigger = Majority

trigger_pixels = 5

teltrig_min_time = 0.5 % [ns]

teltrig_min_sigsum = 0.0 % [mV*ns]

% ----- Readout Signal-----

fadc_mhz = 500 % MHz sampling rate -> 2 ns bins

fadc_bins = 120 % Number of time intervals simulated for ADC.

peak_sensing = 1 % 0|1 (default: 0, sum, 1: peak)

fadc_ac_coupled = 1 % 1 = AC coupled , default 1.

fadc_pulse_shape = astri_slow_shaper_50ns.dat

fadc_pedestal = 971.0 % Per time slice

fadc_amplitude = 62.5 % The peak amplitude in a time slice for high gain 57.5*1.08696

fadc_noise = 1.69 % Per time slice (high gain)

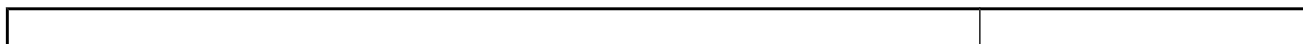
fadc_sensitivity = 1. % default 1.

fadc_var_sensitivity = 0. % default 0.02

fadc_lg_amplitude = 3.125 % The peak amplitude in a time slice for low gain. 1/20 of HG

fadc_lg_noise = 0.3125 % Again per time slice (low gain). noise = 1/10 of pe

fadc_lg_pedestal = 961 % (default = -1: use fadc_pedestal instead)





CONCLUSIONS

--	--



REFERENCES

[1] Bernlöhner K., *Astroparticle Physics* 30 (2008)

[2] Bernlöhner K., "Sim_telarray user guide" (2001)

[3] Di Pierro F. et al., "The CTA telescope simulation software: sim_telarray", (2014)
ASTRI-MC-OATO-5000-006

[4] Canestrari R. et al., "Optical Design Document", (2012) ASTRI-DES-OAB-3500-002

[5] Di Pierro F. et al., "Calculation of nightsky background photoelectron rate in an individual pixel", (2014) ASTRI-MC-OATO-5000-012

